Title
THE USE OF SYMMETRY IN THE TEM ANALYSIS OF PRECIPITATE MORPHOLOGIES

Authors
Dahmen, U.
Westmacott, K.H.

Publication Date
1986-02-01

Lawrence Berkeley Laboratory
UNIVERSITY OF CALIFORNIA

Materials & Molecular Research Division

Presented at the Material Society Meeting,
Boston, MA, December 2-7, 1986

THE USE OF SYMMETRY IN THE TEM
ANALYSIS OF PRECIPITATE MORPHOLOGIES

U. Dahmen and K.H. Westmacott

February 1986

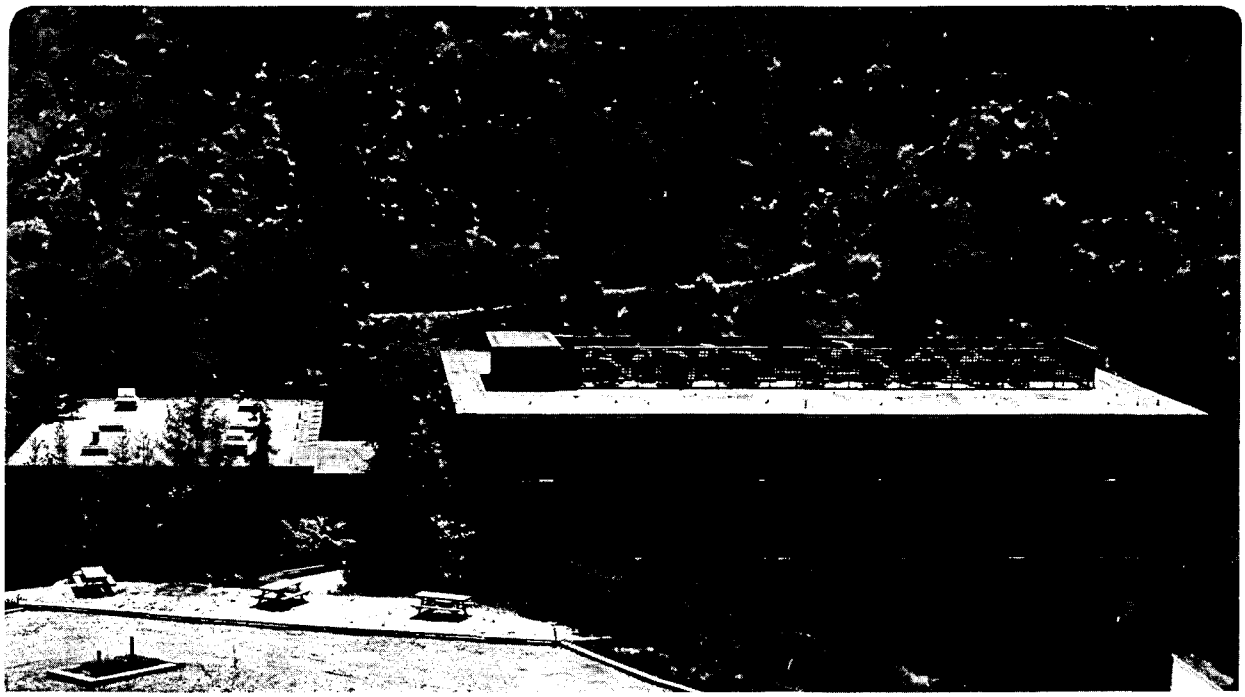

Prepared for the U.S. Department of Energy under Contract DE-AC03-76SF00098

DISCLAIMER

THE USE OF SYMMETRY IN THE TEM ANALYSIS OF PRECIPITATE MORPHOLOGIES

U. DAHMEN AND K.H. WESTMACOTT
Materials and Molecular Research Division, Lawrence Berkeley Laboratory, Department of Materials Science and Mineral Engineering, University of California, Berkeley, CA 94720

ABSTRACT

This study points out how symmetry properties inherent in precipitation reactions can be exploitet to facilitate and improve the accuracy of a morphological analysis by TEM. A method is given for the simple determination of the direction and distribution of needle precipitates and the habit plane of plate precipitates based on the use of symmetry properties of the matrix crystal. The bicrystal symmetry of different orientation relationships between cubic crystals and its connection with observed and equilibrium shapes is illustrated with examples of high resolution micrographs of Ge precipitates in an Al matrix.

INTRODUCTION

In past TEM analyses, symmetry properties of electron diffraction by crystalline solids have been employed only to a limited extent, for example to determine the nature of stacking faults, small dislocation loops or inclusions. Recent advances in convergent beam electron diffraction to determine local crystal structures have made the use of symmetry much more familiar to electron microscopists.

In contrast, symmetry rules have been long-known in the theory of phase transformations[1,2] and in the past decade a group theoretical framework for group-subgroup transitions has been developed. Originally this was applied only to order-disorder transformations where a disordered high-symmetry point phase transforms to a random domain assembly of the

lower-symmetry product phase[3,4]. The role of lattice distortions in forming these domain structures was pointed out later in the context of ferroelastic transitions[5]. Symmetry aspects of large strains as encountered in martensite transformations were treated separately[6], and only recently have some of these concepts been applied to precipitate morphologies, interphase interfaces and martensite variants[7-10]. Most of these previous studies have emphasized the enumeration and prediction of domain, grain or interphase boundaries and concentrated on the symmetry of the factors that led to their formation. However, it is not generally appreciated that the same symmetry principles can be used to facilitate the analysis of such morphologies by TEM.

The present paper will focus on the practical use of crystal symmetry in analyzing precipitate morphologies. Particular emphasis will be placed on needle and plate precipitates in a cubic matrix. Application and observation of symmetries in morphologies and orientation relationships will be illustrated with examples in Al-Ge, Cu-Cr and Fe-N alloys.

DETERMINATION OF THE AXIS OF NEEDLE PRECIPITATES

In order to identify the crystallographic direction of a needle or rod-shaped precipitate in a TEM it is usually necessary to tilt to several different orientations and determine its long axis by trace analysis [11]. Often many crystallographically equivalent variants of the same needle precipitate are present in the same grain. As shown below it is then possible to identify the needle axis from a single micrograph. This type of analysis exploits the crystal symmetry that prescribes the relative orientation of all the variants.

Any two variants of a precipitate are related by a point symmetry operation of the matrix. This is readily apparent from the sequence

of operations shown schematically in Fig. 1: A precipitate is embedded in a matrix crystal (a). A spherical region including the precipitate is cut from the matrix (b), removed (c), rotated, inverted or mirrored by a matrix symmetry operation (d) (here a 90 ° rotation), replaced in the matrix (e) and re-welded (f). The matrix crystal is undisturbed by this sequence because by definition it is invariant under a symmetry operation. However, a new variant of the precipitate has been generated. The number of possible variants is therefore equal to the number of symmetry elements in the point group of the matrix (if translations are ignored).

If however, the precipitate shares one of the symmetry elements of the matrix, then this element will not produce a new variant. In Fig. 1, if the symmetry operation applied in (d) is a 180° rotation it will leave both matrix and precipitate invariant. Thus only those symmetry elements of the matrix that are not shared by the precipitate generate new variants [4,7]. In a morphological analysis needle-or plate-shaped precipitates can be approximated by cylindrical symmetry (∞/mm). A precipitate variant is therefore completely characterized by its axis [hkl] (the axis of cylindrical symmetry). A general axis direction <hkl> in a cubic matrix has 48 variants, or 24 when $\bar{h}\bar{k}\bar{l}$ and hkl are indistinguishable, corresponding to the 48 cubic point symmetry elements and enumerated by the permutations of the 3 indices hkl and their negatives. This is most graphically illustrated in a stereogram, for example an <001> orientation as shown for the general direction <hkl> in a cubic crystal in Fig. 2a. 24 different variants of <hkl> needles are possible if the needle- or cylinder morphology shares none of the

symmetry elements of the matrix. If the needles lie on a {110} mirror plane, i.e. their indices are <hhl>, this mirror is a shared symmetry element and only twelve different variants exist, see Fig. 2b. The same number of variants is found if the needles lie on {001} mirror planes having indices <hk0>, see Fig. 2c. <110> needles lie on both types of mirror and only six variants are possible as shown in Fig. 2d. Only four variants are seen if the needles are along <111> directions (Fig. 2e) and in the simplest case only three variants exist for needles along <001> directions (Fig. 2f).

Each of the variant-generating symmetry operations may be thought of as a specimen tilt in a trace analysis. Needle axes can therefore be measured directly from a single micrograph in an <001> orientation. This is most apparent for <100> needles as illustrated with an Al-Ge alloy in Fig. 3. Of the three variants, one is end-on while the other two are seen at right angles.

<111> needles will give a similar appearance. In an <001> orientation the four variants are projected at right angles on the traces of the {110} mirror planes.

<110> needles form six variants which in an <001> orientation project in two right-angle groups, one aligned with the {100} mirror planes, the other offset by 45°.

These three cases are easily distinguished by inspection and no further measurements are necessary.

The cases of <hk0> and <hhl> precipitates require measuring the angle enclosed by two variants bisected by a {100} mirror. For example in an [001] projection the specific mirror plane (100) bisects the angle

α between the two specific variants $[\bar{h}k0]$ and $[hk0]$. This angle is given by:

$$\cos\alpha = (k^2-h^2)/(k^2+h^2) \qquad (1)$$

Thus the ratio $h^2/k^2 = (1-\cos\alpha)/(1+\cos\alpha)$, where α is measured directly from a micrograph.

The same type of measurement yields the ratio h^2/l^2 for <hhl> precipitates. <hk0> and <hhl> needles are easily distinguishable by the position of their projections with respect to the traces of the {100} mirror planes in the micrograph. As seen from the stereogram in Fig. 2 <hk0> needles have some variants projecting onto the traces of {100} mirror planes whereas <hhl> needles have some variants projecting onto the traces of the {110} mirror planes.

The axis of needles in the general <hkl> direction can be found in a similar manner by measuring the intervariant angles which are bisected by the {100} mirror plane. For a unique solution only three angles $\alpha<\beta<\gamma<90°$ should be used. The indices hkl are then given by:

$$h^2/l^2 = (1-\cos\alpha)/(1+\cos\alpha),\ h^2/k^2 = (1-\cos\beta)/(1+\cos\beta),\ k^2/l^2 = (1\cos\gamma)/(1+\cos\gamma) \qquad (2)$$

Clearly two angles are sufficient and the third maybe used to check the accuracy of the measurement.

An example is given in Fig. 4 which shows an <001> projection of Cr needles in a Cu matrix. The traces of the {100} mirror planes are indicated as dashed lines. The largest intervariant angle smaller than 90° straddling the {100} trace is measured to be $\gamma = 80°$, the next largest angle is $\beta = 27°$ and the smallest angle α is difficult to measure with any accuracy because these variants are steeply inclined to the plane of the projection. Substituting the measured angles β and γ into equation (2) we obtain hkl = 651. This agrees with the original needle

axis-determined by trace analysis(12).

It must be kept in mind that this simplified analysis is valid only for a random distribution of all crystallographic variants of one type of precipitate. If the distribution is not random or more than one type of precipitate is present the analysis becomes ambiguous. The uniqueness of a needle analysis is thus a good test of the randomness of the distribution and whether one or more crystallographic types are present.

An example of the latter case is shown in Fig. 5a with needle precipitates in an Al-Ge alloy seen along an <001> zone axis. If only one type of precipitate needle were present this could be analyzed immediately as <110> precipitates since only projections in <100> and <110> directions exist. However, by reference to the stereograms in Fig. 2 it can be seen that this would also be true if either <111> or <100> needles, or both, were superimposed on the <110> needles. To check for multiplicity in the distribution it is necessary to examine another projection along a direction of no symmetry. Clearly <110> needles alone would show 6 variants, <111> needles would add another 4 variants and <110> needles a further 3 variants. Thus by counting variants in this general orientation* (6,7,9,10 or 13) it is possible to determine uniquely the multiplicity of the distribution. Al-Ge alloys provide an example for this. In an <001> projection (Fig. 5a) the distribution is that of <110> needles. In a general orientation of no symmetry (Fig. 5b) 9 variants can be counted. The distribution is thus a mixture of six <110> and three <100> needles.

*(Care must be taken to avoid any symmetry elements perpendicular to, in the plane of this projection. For example a <123> orientation containing the threefold <111> axis is unsuitable since it may project all three variants generated by this axis in the same direction).

A non-random, or biased, distribution of needles may be detected if one or several of the variants are missing. This may be the case if the "nucleation function (4) is of low symmetry; for example if a uniaxial stress is applied during nucleation, the (cylindrical) symmetry of the stress favors some nuclei over others, leading to a biased distribution. The presence of such a bias is most easily found in an orientation of no symmetry since in a high symmetry zone axis many of the variants are indistinguishable.

DETERMINATION OF THE HABIT PLANE OF PLATE PRECIPITATES

The method outlined above is not limited to needles in a cubic matrix but can be applied to any crystallographic linear features such as dislocation lines or plane intersections and can easily be extended to non-cubic matrices. For example the crystallographic indices of planar features such as plate precipitates or stacking faults can be obtained in exactly the same manner as the direction of needle precipitates if a foil with known surface orientation is used. Thus a <uvw> foil surface of a cubic matrix will intersect all different variants of a general {hkl} plane in 24 different directions. A precise {001} surface can therefore be used for accurate measurements of the angles between plane traces and, by use of equ. 2, for determination of the crystallographic indices {hkl} A foil surface normal to an axis of no symmetry can be used to find the number of variants present from the number of different intersections. The displacement fringe contrast commonly observed in TEM images of thin plates is parallel to the intersection of the habit plane with the surface even if the precipitate plates are completely contained in the foil as could be the case for small precipitates or

thick foils. The reverse process, the exact determination of the foil surface orientation from the directions of intersection with low-index planar features such as stacking faults, has been described and used previously [13], and the intersection of two known surfaces with a planar feature such as the habit plane of a precipitate is well-known as two-surface trace analysis.

Often additional features introduced by crystal symmetry can be used to analyze precipitate morphologies. An example is shown in Fig. 6 where large plate precipitates of γ' with fcc Fe sublattice in bcc Fe-N are intersecting a thin foil at an angle. Two sets of striations are visible in the same planar interface. This type of linear feature in an interface usually indicates an invariant line direction [14]. The vertical plate thus contains two variants of the invariant line, i.e. the corresponding parts of the plate are two variants of the precipitate. Since both variants clearly share the same habit plane and since any two variants are related by a symmetry operation of the matrix (see Fig. 1) it follows that the habit plane must have at least one symmetry element in common with the matrix, e.g. it must be parallel or perpendicular to a mirror plane or rotation axis. From Fig. 2 it can be seen that this restricts the habit plane to the type {hk0} if the mirror or rotation axis is of the 001 type and {hhl} if the mirror or rotation axis is of the 110 type. In the present case the two degenerate variants were found to be related by an {001} mirror and the habit plane is therefore of the type {hk0}.

In order to determine the exact orientation, i.e. the ratio of h to k, the angle between two {hk0} plates seen edge-on in an <001> foil orientation can be measured accurately. As seen in Fig. 7a two {hk0}

plates usually group together in a V-shaped morphology. A {110} mirror plane of the matrix bisects the angle of 42° subtended by the two variants. The habit plane is therefore {940} and further investigation reveals the complete morphology as butterfly-shaped with each wing consisting of two degenerate variants. A schematic of this morphology is shown in Fig. 7b with the location of the relevant matrix symmetry elements indicated.

SYMMETRY OF PRECIPITATE SHAPES

The simple analysis described in the previous sections approximates a precipitate morphology by a characteristic direction or habit plane. A true morphological analysis must characterize the three-dimensional shape of a precipitate and its orientation relationship with the matrix. As has been pointed out recently, the orientation relationship and the equilibrium shape of a precipitate have the same symmetry, namely that of the intersection of the point groups of matrix and precipitate[7]. It is therefore important to determine the orientation relationship and as an example a high resolution image of <100> needle precipitate of Ge seen end-on in <001> Al matrix is shown in Fig. 8. The orientation relationship is now easily recognized as <110> Ge // <100> Al (the needle axis) and {111} Ge // {100} Al. Facets on the {111} Ge faces of this needle give it a diamond shaped cross section in contrast to the cylindrical symmetry assumed earlier. Since the fourfold symmetry of the matrix in this orientation is lost and only the 2/m axis common to matrix and precipitate survives, 2/m (monoclinic) is the symmetry of the orientation relationship and of the equilibrium particle shape. This is clearly evident in the image where the twofold symmetry is disturbed

only by a twin in the particle. At the twin the particle outline contains a jog. The orientation relationship of the twin is different from the rest of the particle with <110> Ge // <100> Al as before but {111} Ge 38.9 ° from {100} Al.

It is interesting to note that the primary orientation relationship is not a symmetry-dictated extremum[10], i.e. any relative rotation of the two lattices around the common 2/m axis such that {111} Ge and {100} Al are no longer parallel can occur without destroying any common symmetries. Indeed, small deviations from parallelism of {111} Ge and {100} Al were found in such twinned particles except when the twin plane was the particular {111} Ge plane that was parallel to the {100} Al plane. An example of such a particle is shown in Fig. 10. The twin plane is exactly parallel to the {100} Al mirror plane relating the Ge crystal and its twin. By the definition in Fig. 1 of the generation of variants, the Ge crystal and its twin are two variants of the same orientation relationship. Seen as a symmetry element the twinning adds pseudo-mirror symmetry to the precipitate; in fact the $\Sigma 3$ coincidence site lattice common to two twin-related crystal has true mirror symmetry across the twin plane. For this $\Sigma 3$ CSL the alignment of {111} Ge with {100} Al is therefore a symmetry-dictated extremum in the orientation relationship as seen for example in Fig. 9. Again the shapes of the individual twins have approximately 2/m symmetry elongated along the common low-index planes {111} Ge // {100} Al by about 3:1.

Other orientation relationships with higher than monoclinic symmetries were found. Fig. 10 shows a needle with its axis along <110> Ge // <100> Al and {110} Ge // {110} Al. The symmetry of this orientation

relationship, and hence the equilibrium particle shape, is orthorhombic, mmm with the mirror planes along the major axes of the particle. This is a symmetry-dictacted extremum. Note that this needle has no {111} Ge facets but is flat and parallel-sided on the common {110} plane. Twins traversing the particle diagonally have a different, non-rational orientation relationship with <110> Ge // <100> Al and {100} Ge 25.5° from {100} Al.

The particle shown in Fig. 11 has an orientation relationship with tetragonal (4/mmm) symmetry since <110> Ge // <100> Al and {100} Ge // {100} Al, a symmetry-dictated extremum. The common fourfold axis is normal to the flat face of the particle whose sides have {111} Ge facets. Its equilibrium shape would be a square plate normal to the common fourfold axis with edges bounded by {111} Ge facets. Twinning in the Ge again leads to an irrational orientation relationship with <110> Ge // <100> Al and {100} Ge 19.5° from {100} Al. Because of the common fourfold axis the four twin variants have the same type of orientation relationship and all four twins are equally likely to occur. In the <110> Ge projection in Fig. 11 two twins are apparent, the other two would be inclined to this orientation.

The cube-cube orientation relationship with $m\bar{3}m$ symmetry has also been observed in Al-Ge [15] and here the morphology of hexagonal or triangular plates reflects the common 3 fold axis. However these particles do not display full cubic symmetry because of the lower symmetry of the mechanism of volume accommodation by vacancy loops (∞/mm). The precipitate equilibrium shape only has the symmetry that is common to all factors involved in their formation, given here by the intersection of the

orientation relationship symmetry ($m\bar{3}m$) with the accommodation mechanism symmetry (∞/mm), i.e. ($\bar{3}m$).

SUMMARY AND CONCLUSIONS

The use of crystal symmetry in the TEM analysis precipitate morphologies has been illustrated with examples of needle- and plate-shaped precipitates in different alloy systems. In a simplified analysis the precipitates are characterized by a crystallographic direction, the needle axis or habit plane normal. The matrix single crystal symmetry can then be used to determine this direction from a single micrograph showing a projection of all precipitate variants along a high-symmetry axis. A complete morphological analysis must consider the bicrystal symmetry of the orientation relationship between matrix and precipitate. The equilibrium shapes corresponding to different orientation relationship are compared with shapes of Ge precipitate in an Al matrix observed by high resolution electron microscopy.

ACKNOWLEDGEMENTS

We thank J. Bierach for preparing the Al-Ge samples and C. Nelson for taking the ARM micrographs in Figs. 9-11. This work is supported by the Director, Office of Energy Research, Office of Basic Energy Sciences, Materials Sciences Division of the U.S. Department of Energy under Contract No. DE-AC03-76SF00098.

REFERENCES

1. L.D. Landau and E.M. Lifshitz, "Statistical Physics", Addison Wesley.
2. J.M. Sanchez, D. Gratias and D. DeFontaine, Acta Cryst. A38, 214 (1982).
3. G. VanTendeloo and S. Amelinckx, Acta Cryst. A30, 431 (1974).
4. D. Gratias, R. Portier and M. Fayard, Acta Cryst. A35, 885 (1979).
5. C. Boulesteix, Phys. stat. sol. (a) 86, 11 (1984).
6. J.W. Cahn, Acta Met. 25, 721 (1977).
7. J.W. Cahn and G. Kalonji, Proc. Int. Conf. Solid-Solid Phase Transf., Pittsburgh, (1981), p. 3.
8. R. Portier and D. Gratias, J. de Phys., Coll. C4 43, 4 (1982).
9. V.K. Wadhawan, Mat. Sci. Forum 3, 91 (1985).
10. A. Ben Lamine, R. Portier, J.P. Senateur and F. Reynaud, Scr. Met. 19, 63 (1985).
11. J.W. Edington, Practical Electron Microscopy in Materials Science, MacMillan Philips Technical Library, Philips, Eindhoven (1975).
12. G.C. Weatherly, P, Humble, D. Borland, Acta Met. 27, 1815 (1979).
13. S.M. Allen, 10th. Int. Congr. Electr. Micr. (1982), p. 353.
14. J.M. Lang, U. Dahmen and K.H. Westmacott, Phys. stat. sol. (a) 75, 409 (1983).
15. U. Köster, Mat. Sci. Eng. 5, 174 (1969).

FIGURE CAPTIONS

Fig. 1. Sequence of hypothetical operations relating the two precipitate variants shown in (a) and (f); a spherical volume including the precipitate is cut from the matrix (b), removed (c), rotated mirrored or inverted (d) and replaced in the matrix (e). Since the operation in (d) produces an identical matrix orientation, a single crystal is restored (f) with the precipitate in a new orientation.

Fig. 2. <001> stereograms of a cubic crystal showing distribution of a general needle direction <hkl> with 24 variants in (a), <hhl> needles (12 variants) in (b), <hk0> needles (12 variants) in (c), <110> needles (6 variants) in (d), <111> needles (4 variants) in (e) and <100> needles (3 variants) in (f). Each distribution gives a characteristic appearance in an <001> projection allowing the determination of h,k and l from measurement of the angles α, β and γ shown in (a).

Fig. 3. Distribution of <100> needle precipitates in Al-3% Ge alloy quenched and aged 1h at 240°C, seen here in <001> projection.

Fig. 4. Distribution of <651> needle precipitates in Cu-0.3%Cr alloy quenched and aged 18h at 700°C, seen here in <001> projection.

Fig. 5. Al-3% Ge alloy quenched and aged 1h at 240°C showing precipitates projecting in <100> and <110> directions when projected along <001> (a); 9 different nedle directions are counted (see marks)

in a projection of no symmetry (b). The needles are therefore of <110> and <100> but not <111> type.

Fig. 6. Inclined plate precipitates of γ'-Fe_4N in Fe-N alloy quenched and aged 3 min in-situ at 300° C. The vertical plate contains two sets of finely spaced parallel striations and intersects the foil surfaces in a straight line. The two plate variants corresponding to the two sets of striations must therefore lie on {hhl} or {hk0} planes.

Fig. 7. (a) V-shaped group of two variants of γ' Fe_4N plates seen edge-on in a <100> orientation, enclosing an angle of 42°. Together with the information from Fig. 6 this allows an accurate determination of the habit plane as {940}. A schematic of the complete morphology is shown in (b).

Fig. 8. High-resolution image of <110> Ge/<100>Al needle precipitate in Al-3Ge seen edge-on. The symmetry of the orientation relationship {111}Ge/{100}Al, is monoclinic (2/m). The needle is facetted on {111} Ge planes, and apart from the narrow twin, exhibits twofold rotational symmetry in this projection. The orientation relationship of the twin is different but maintains 2/m symmetry.

Fig. 9. High-resolution image of <110> Ge/<100>Al precipitate seen end-on with the same orientation relationship as before but twinned on the {111}Ge plane that is parallel to {100}Al. This is a symmetry-dictated extremum for the $\Sigma 3$ coincidence site lattice of the Ge precipitate.

Fig. 10. <110>Ge/<100>Al needle seen end-on with {110}Ge/{110}Al, an orientation relationship with orthorhombic (mmm) symmetry at a symmetry-dictated extremum. Note the approximate mirror symmetry of the shape in this projection with facets on the common {110} planes, disturbed only by the diagonal twins.

Fig. 11. High resolution micrograph of a Ge plate seen edge-on along the common <110>Ge/<100> direction. This orientation relationship, with {100}Ge/{100}Al, has tetragonal (4/mmm) symmetry which is also reflected in the shape of the particle. The common fourfold axis is normal to the flat face of this precipitate.

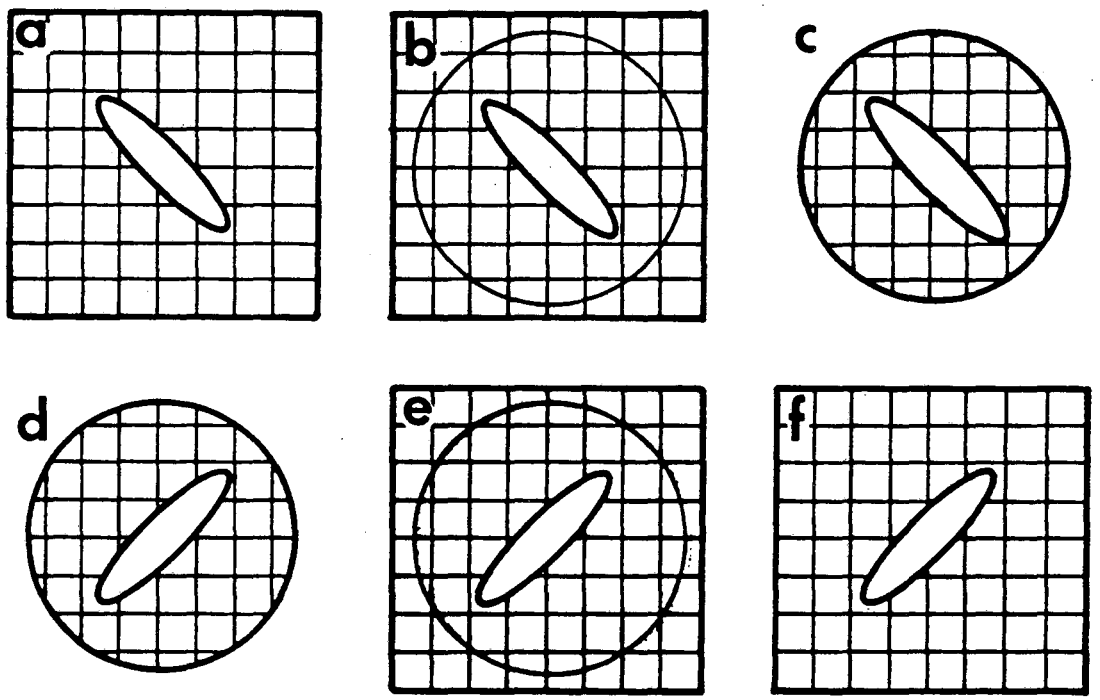

XBL 8511-4781

Fig. 1

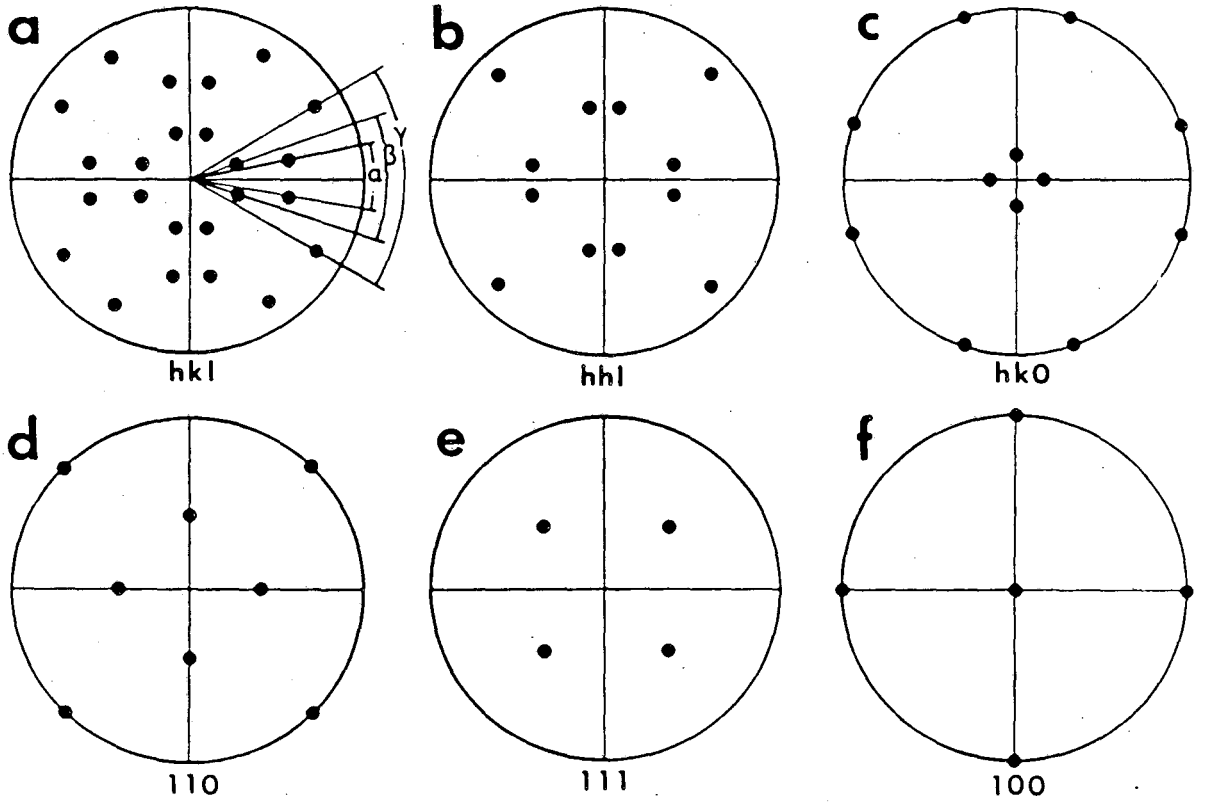

XBL 8511-4783

Fig. 2

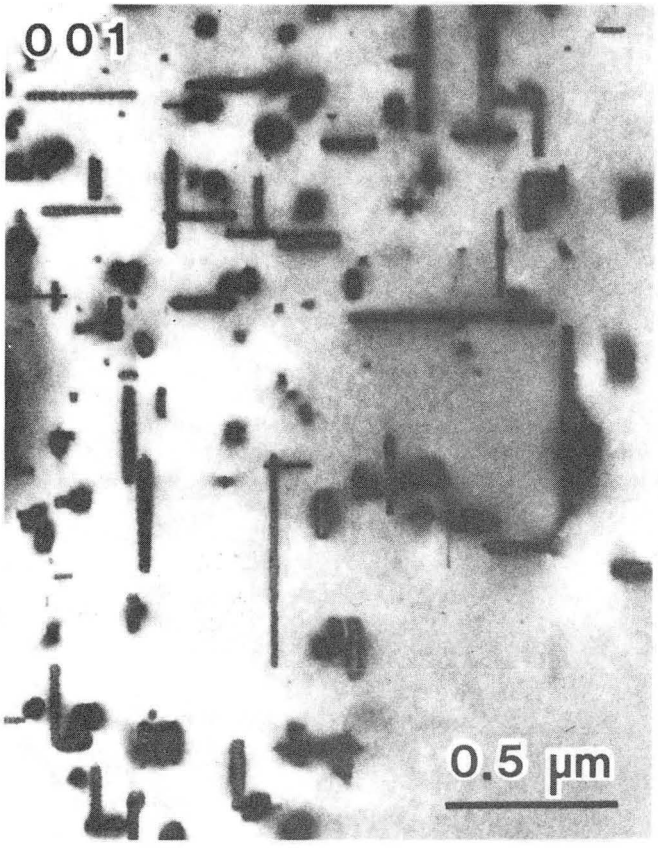

XBB 861-298

Fig. 3

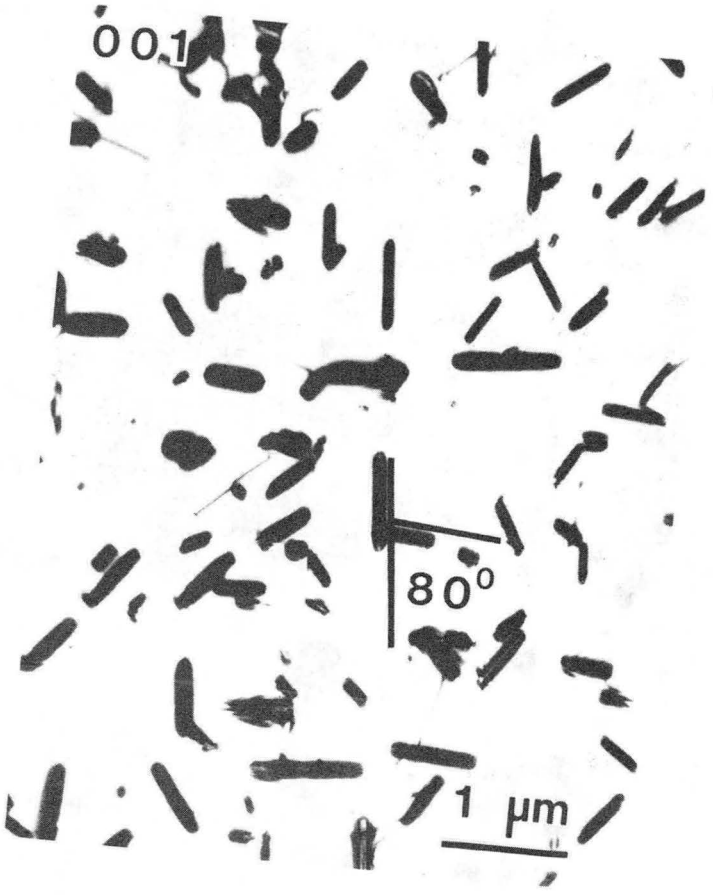

XBB 861-299

Fig. 4

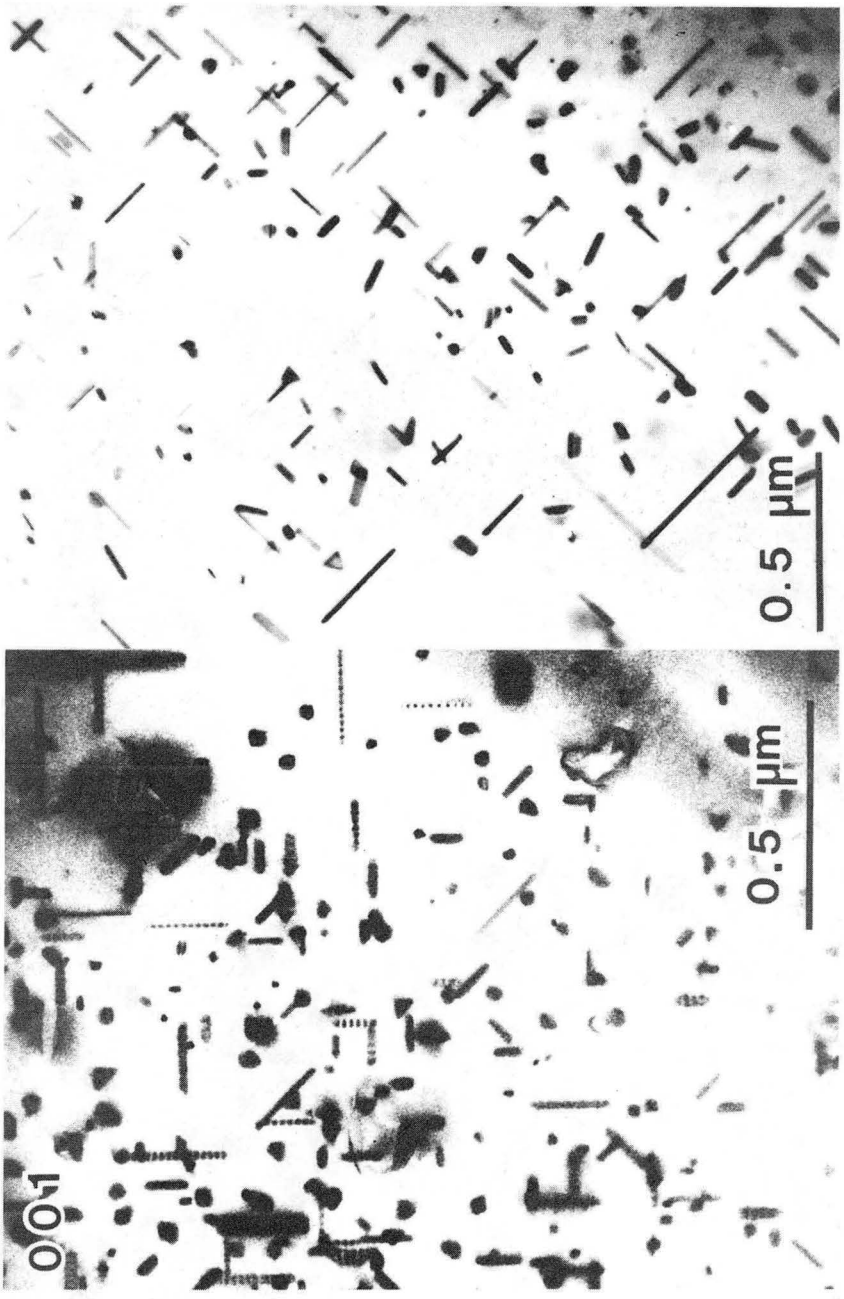

XBB 861-300

Fig. 5a-b

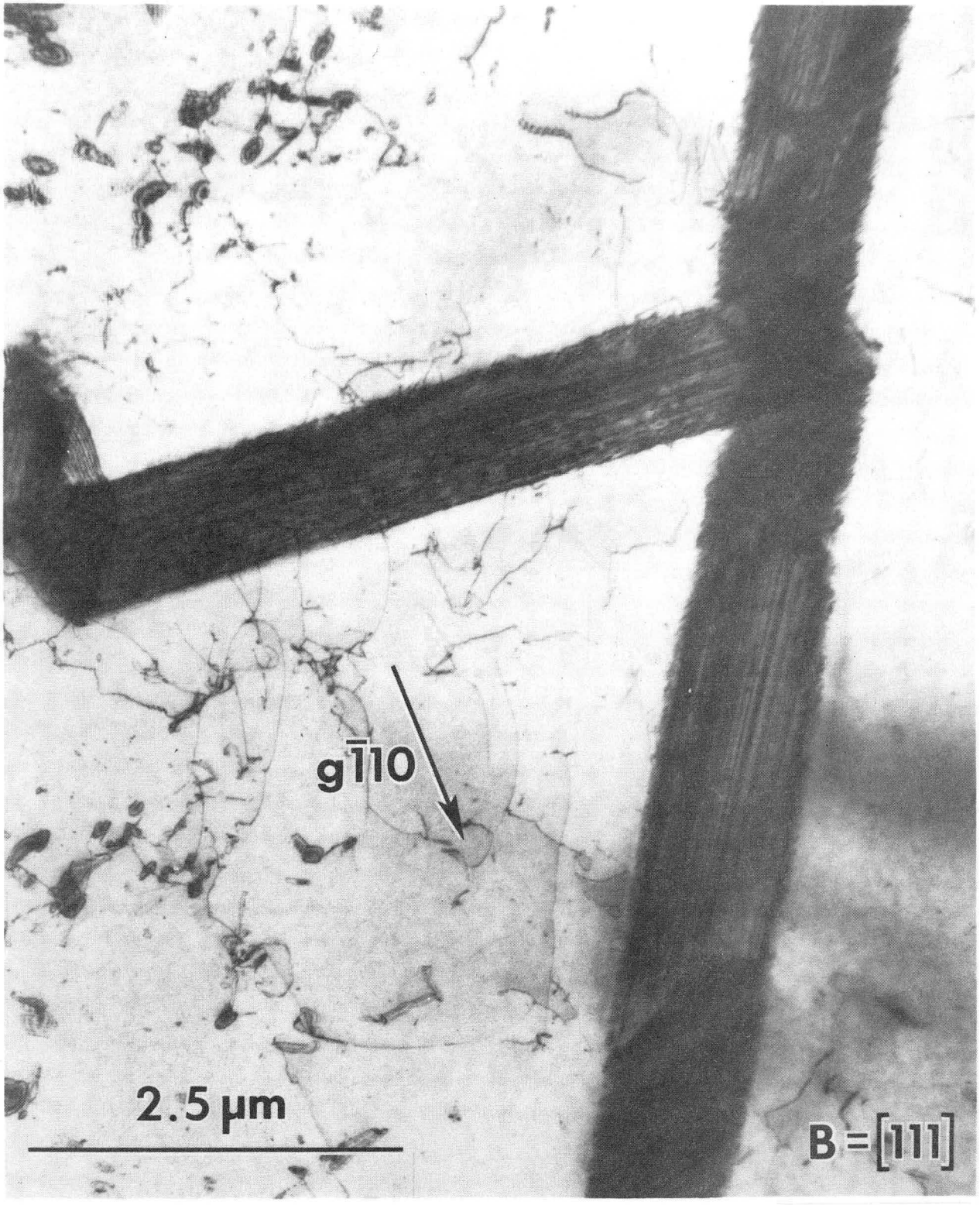

XBB 834-3797

Fig. 6

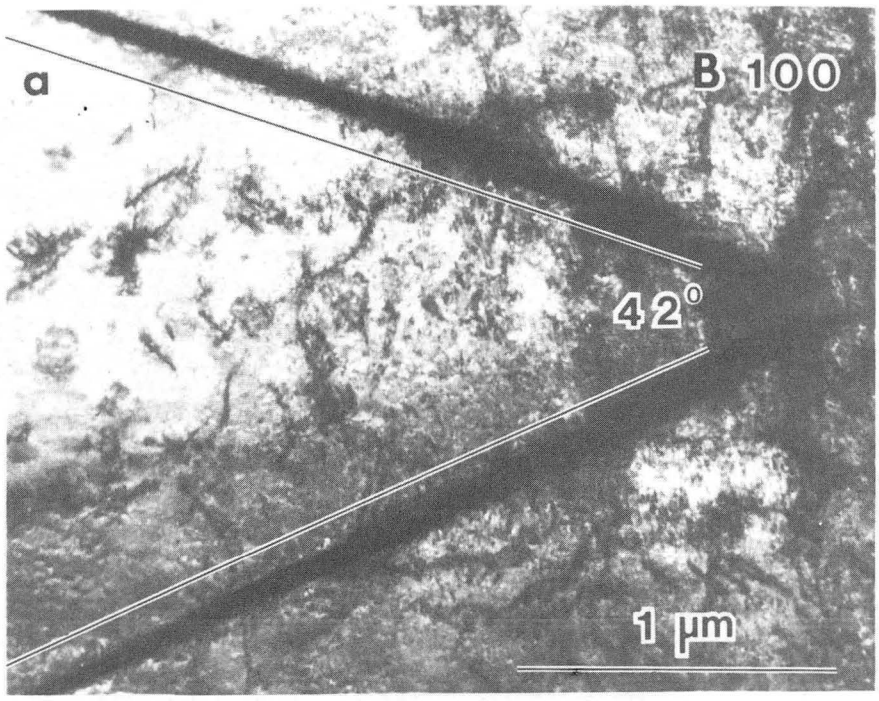

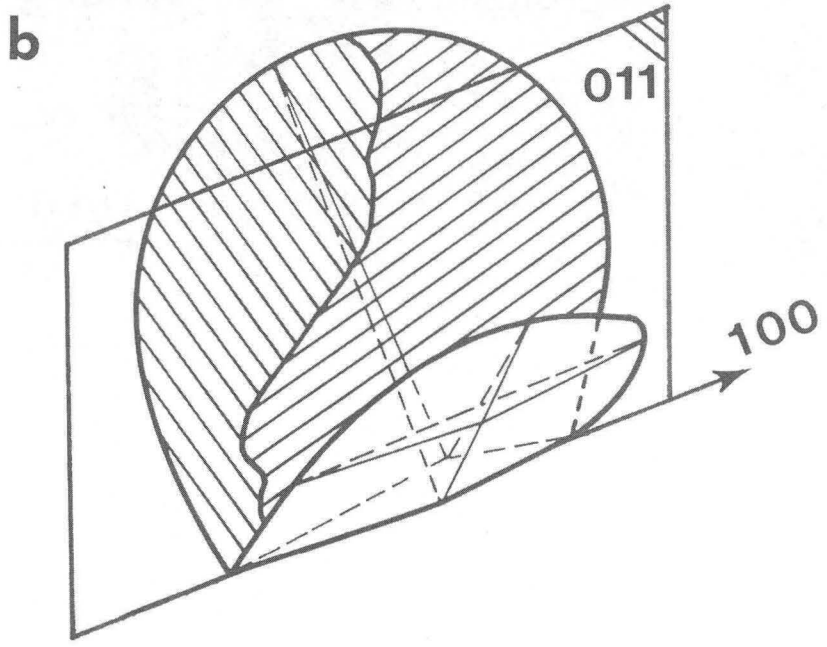

XBB 861-301

Fig. 7a-b

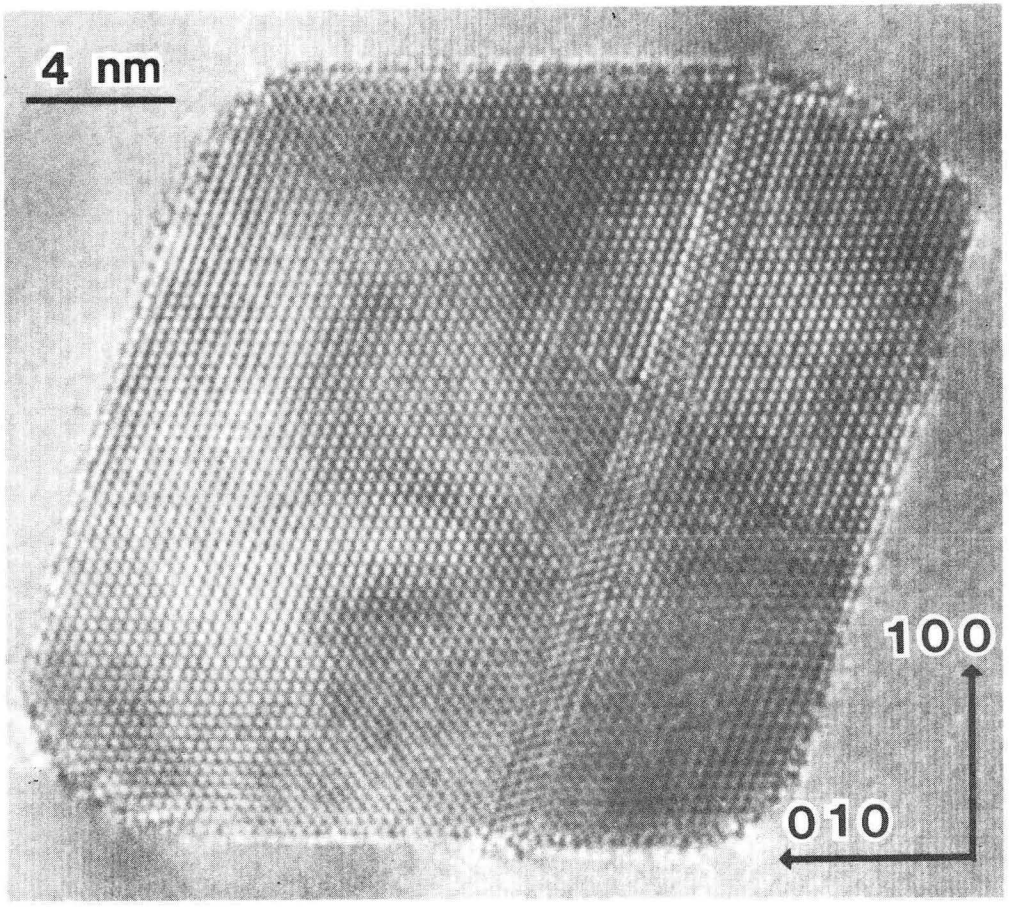

XBB 861-302

Fig. 8

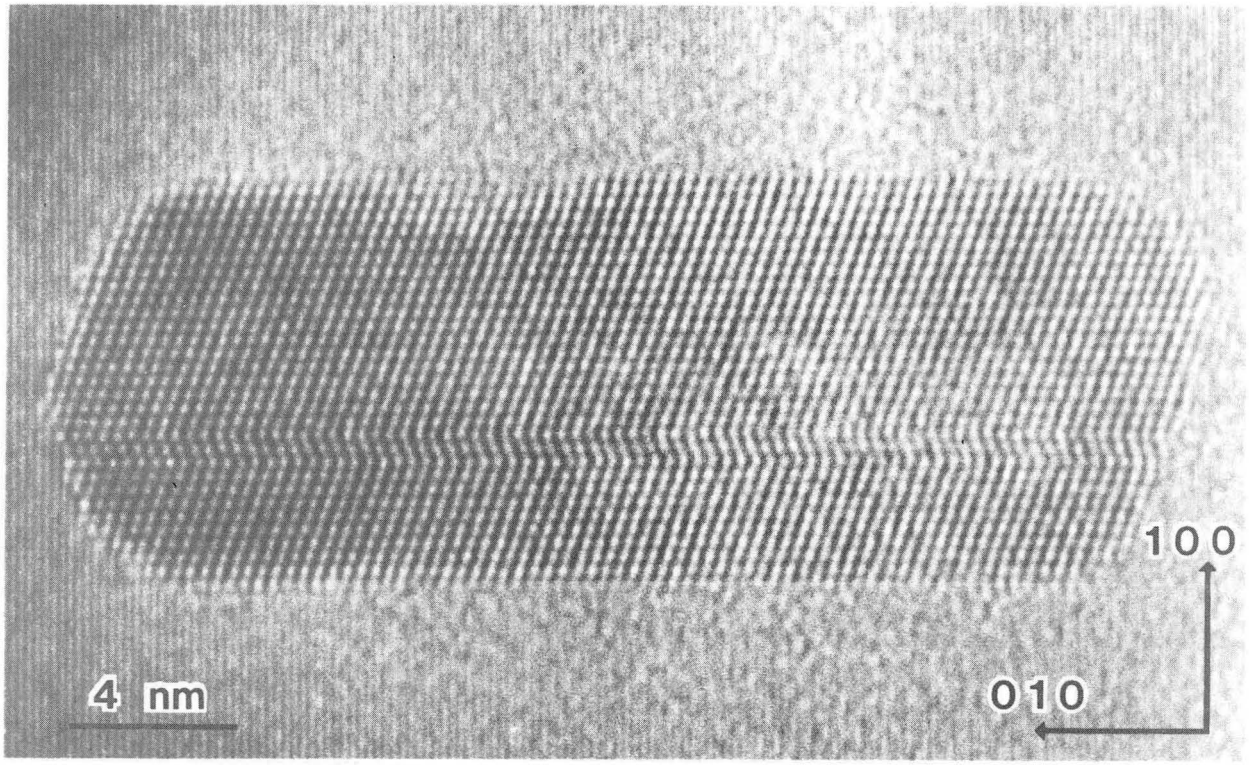

XBB 861-303

Fig. 9

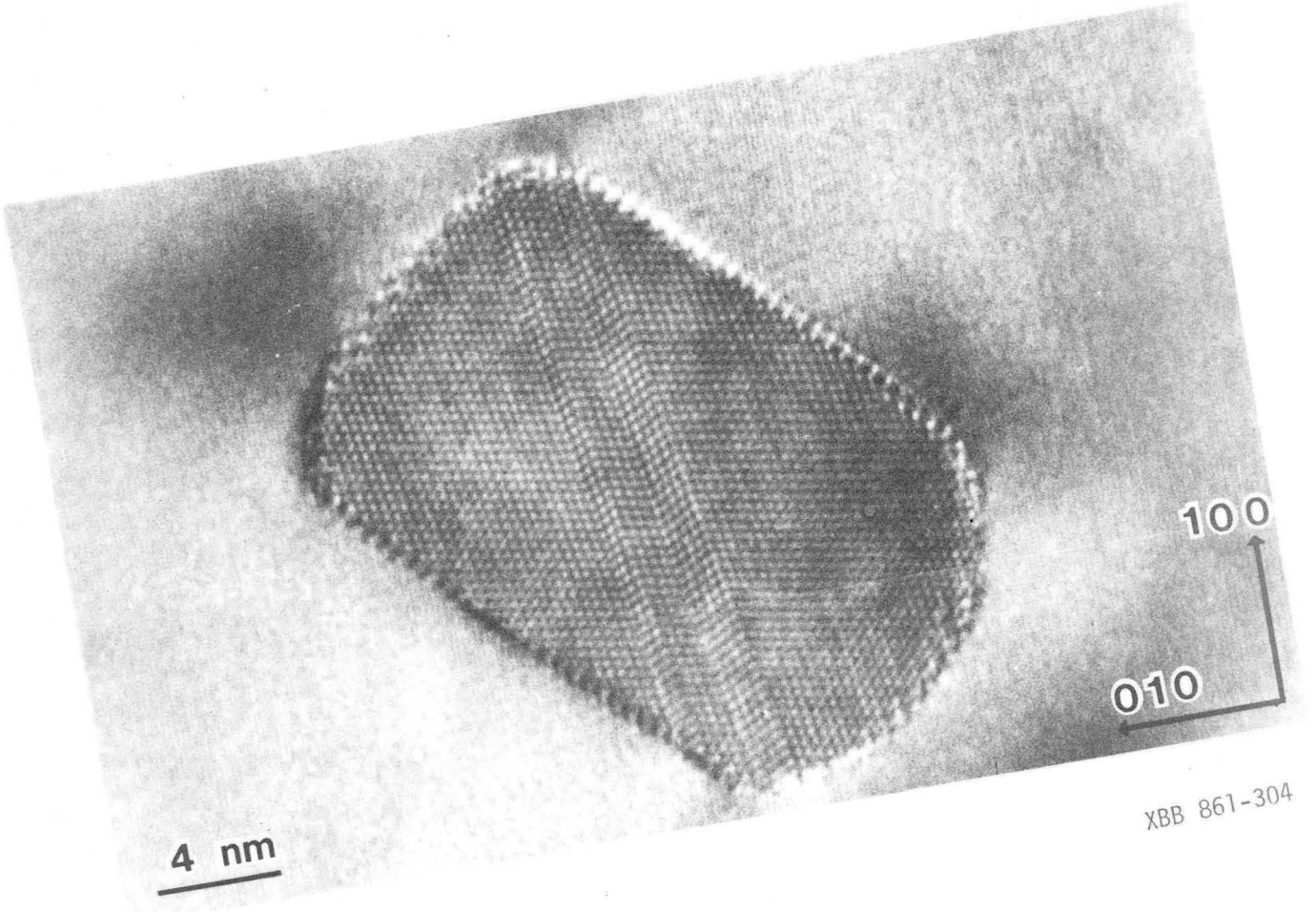

XBB 861-304

Fig. 10

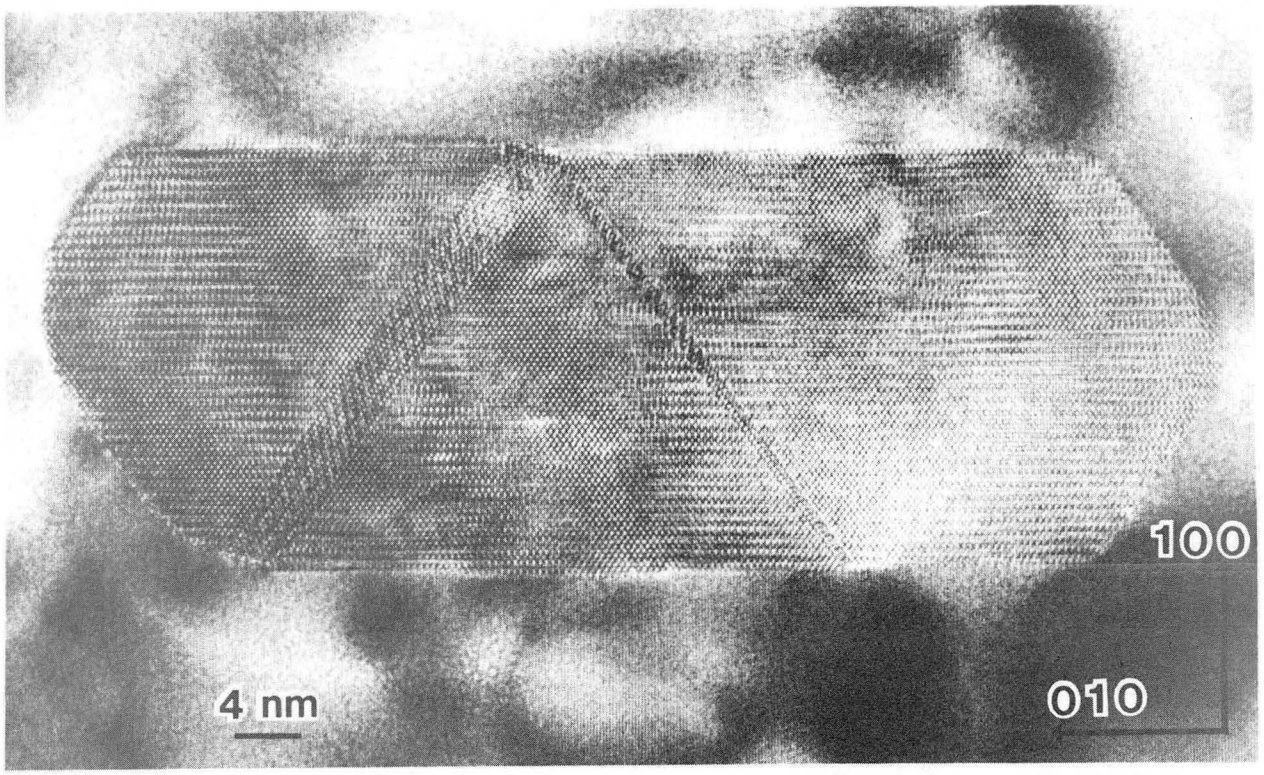

XBB 861-305

Fig. 11

LAWRENCE BERKELEY LABORATORY
TECHNICAL INFORMATION DEPARTMENT
UNIVERSITY OF CALIFORNIA
BERKELEY, CALIFORNIA 94720